arXiv:2606.27355v1 [cs.RO] 25 Jun 2026

RouterVLA: Turning Smoke Tests into Supervision for Heterogeneous VLA Selection

Xingyu Ren[1] *, **Chugang Yi**[2] *, **Ge Ma**[3] †, **Youran Sun**[2] ‡

[1]The Chinese University of Hong Kong
[2]University of Maryland, College Park
[3]Tsinghua University

Abstract

We study whether pre-deployment evaluation rollouts can be reused to supervise policy selection. Robot teams routinely smoke test candidate vision-language-action (VLA) policies, then compress those trials into a global winner. RouterVLA evaluates this idea with outcome-disjoint cross-fitting: recorded probes build a profile for each frozen expert, and a separate trial scores the selected expert without entering its profile. Across 34,752 LIBERO-Plus rollout records, a transparent probe-success rule raises held-out success from 0.4686 to 0.6149, a +14.64pp gain. Under the scalar-only profiles studied here, learned scorers are statistically indistinguishable from this rule, showing that commissioning carries the routing value while extra scalar scorer capacity does not create it. Reusing the scored trial inflates the measured gain by 1.87×, so credible ledger routing needs outcome separation; model scaling improves individual policies, while commissioning-aware routing improves the system built from them.

Introduction

A robotics team usually tests a vision-language-action (VLA) policy on the target setup before deployment. This commissioning phase may include a handful of smoke tests for each candidate checkpoint. The usual workflow then compresses this evidence into one number, chooses the best average performer, and uses that policy everywhere. Commissioning is treated as a cost paid before deployment. We ask whether it can instead become supervision.

That question matters because a policy pool is rarely redundant. One expert may tolerate a camera shift but fail after an object is moved; another may be slower yet more reliable from difficult robot states. LIBERO and LIBERO-Plus make this dependence visible, since policy rankings change across task suites and controlled perturbations [Fei et al. 2025, Liu et al. 2023]. A global average hides the information needed to choose among complementary experts.

Scaling laws have made one axis of progress familiar by showing how more data and capacity can make a single model broader [Kaplan et al. 2020]. Robot learning follows that axis through broader pretraining and stronger adaptation. OpenVLA and $\pi_{0.5}$ illustrate how far this approach has advanced [Kim et al. 2024, Physical Intelligence et al. 2025]. Deployment creates a second axis. Even as individual policies improve, a team may already possess foundation checkpoints, fine-tuned variants, and task specialists whose strengths only partially overlap. *Model scaling improves the experts; deployment scaling improves the system built from them.* Commissioning-aware routing connects these two axes by recovering conditional value from policies that already exist.

We study the simplest version of this idea for repeated use. For a target task under a specified perturbation, the system runs B probes per available expert, summarizes the observations, and chooses one expert for a scored execution. The probes may reveal success, rollout length, duration, and termination behavior. The scored outcome is unavailable when the choice is made. This setting is natural for a station, task configuration, or operating condition that will be used repeatedly after an initial qualification phase. It is not zero-probe routing to a previously unseen condition.

Retrospective evaluation makes the problem deceptively easy. If the rollout used to score a choice also contributes to the expert profile, the selector can exploit an outcome proxy rather than predict a disjoint execution. The issue is subtle because a complete ledger contains every expert's outcome, including counterfactuals that a deployed system would never observe. We therefore treat outcome separation as part of the problem definition, not as a reporting detail.

RouterVLA evaluates this question on a fixed LIBERO-Plus perturbation ledger. The study contains 34,752 valid rollout records, 398 variants, 28 heterogeneous experts, and four recorded trials per included variant–expert pair. In the primary 3-to-1 cross-fit, three trials form the commissioning profile and the remaining trial scores the selected expert. Rotating the scored trial yields 1,592 evaluation rows. Learned scor-

*Equal contribution.
†gema.academic@outlook.com
‡syouran0508@gmail.com

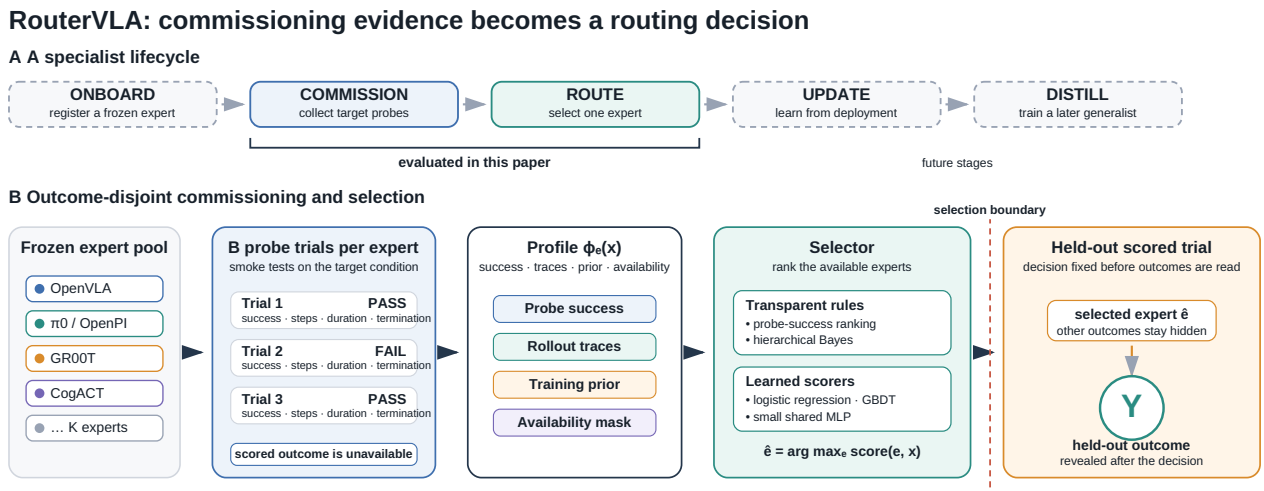

Figure 1: **RouterVLA turns commissioning evidence into an outcome-disjoint expert choice.** Panel A places the evaluated Commission–Route link inside a longer specialist lifecycle. Panel B shows the decision boundary. Probe trials form per-expert profiles, a transparent or learned selector chooses one expert, and the held-out outcome is revealed only afterward. Update and distillation are future stages, not claims of the present study.

ers are trained leave-one-suite-out, while every method uses the same candidate masks and trial-disjoint evidence.

The answer is simpler than we expected. Three probes per expert reveal substantial conditional value, and a transparent probe-success rule improves held-out success from 0.4686 to 0.6149. Logistic regression, GBDT, and a small MLP use richer profiles, yet all remain in the same statistical band. GBDT's +0.38-percentage-point difference from the probe-success rule has 95% CI $[-0.88, +1.57]$. The operational gain comes from conditioning on the target, not from increasing scorer capacity. The protocol also matters, since allowing same-trial reuse raises the measured gain by 1.87× and reaches the realized hindsight upper bound.

The paper makes four contributions:

- **A commissioning-aware formulation.** We define repeated-use VLA selection with an explicit boundary between probe evidence and the scored execution.
- **An outcome-disjoint empirical study.** Across 398 LIBERO-Plus variants and 28 frozen experts, we quantify how much conditional value sparse probes add beyond one global policy.
- **A scoped sufficiency result.** Under equal three-probe budgets with scalar-only profiles, binary probe success saturates the available routing signal. Learned scorers are predictive, but their extra scalar features do not reliably change the selected expert once success evidence is present.
- **An evaluation and design diagnosis.** We measure same-trial optimism, probe cost, shortlist trade-offs, ties, and layout failures. The results motivate active evidence collection and observation-conditioned routing.

We view the measured Commission–Route link as the first stage of a longer specialist lifecycle. A future system can add new experts, decide which ones need additional probes, update beliefs from routed executions, and eventually curate multi-teacher data for a later generalist through distillation [Hinton et al. 2015]. Those stages require new experiments; the present result establishes the control signal they would build on. Commissioning is not merely overhead. It is the first measurement in a system that learns how to use its experts.

Related Work

Routing among robot policies. Several recent systems treat a policy pool as a resource rather than collapsing it into one checkpoint. RoboRouter retrieves semantically similar historical tasks and uses accumulated execution records to choose among heterogeneous manipulation policies [Chen et al. 2026b]. MoIRA routes language instructions to modular robot experts through text similarity or a language model [Kuzmenko and Shvai 2025], while MergeVLA changes the VLA architecture so task-specific adapters and action experts can be selected or merged [Fu et al. 2025]. A similar evidence-limited routing problem appears in LLM serving, where systems choose among models per query under quality and cost constraints [Ong et al. 2024]. These methods use task semantics, instruction text, model weights, or preference data. RouterVLA isolates a different question: after a target condition receives a controlled probe budget, how much of the next exe-

cution can be predicted from black-box feedback when the scored outcome is explicitly excluded from the profile? The emphasis is therefore commissioning evidence, outcome-disjoint measurement, and probe cost rather than semantic task retrieval or model-internal routing.

Algorithm selection and limited-budget evaluation. Algorithm selection asks how to choose a solver from a portfolio using information available before the run [Rice 1976]. Auto-WEKA and Auto-sklearn extend that view to machine-learning pipelines, while Hyperband and related racing procedures allocate limited resources to identify promising configurations [Feurer et al. 2015, Li et al. 2018, Thornton et al. 2013]. Our probes play a similar role, but they are full robot executions rather than cheap descriptors or partial learning curves. That cost makes two questions inseparable: which expert should execute, and how much evidence should be collected before choosing? The use of sampled outcomes as supervision also connects to policy-gradient reinforcement learning, where REINFORCE estimates updates from realized returns [Williams 1992]. Here the sampled outcomes rank frozen experts for one target condition rather than update a policy. Offline policy evaluation also studies decisions from logged interactions [Jiang and Li 2016, Thomas and Brunskill 2016]; here the target is narrower, because explicit probe trials condition a one-step expert choice and the scored row must remain outside that evidence.

VLA shifts, adaptation, and composition. VLA research has progressed from transformer control policies such as RT-1 to web-pretrained VLA transfer, cross-embodiment robot data, and open generalist policies such as Octo and OpenVLA [Brohan et al. 2023a,b, Kim et al. 2024, Octo Model Team et al. 2024, Open X-Embodiment Collaboration et al. 2024]. Fine-tuned OpenVLA variants and the π_0 to $\pi_{0.5}$ line extend that single-policy axis [Black et al. 2025, Kim et al. 2025, Physical Intelligence et al. 2025], while LIBERO-style benchmarks expose how performance changes under task and observation shifts [Fei et al. 2025, Liu et al. 2023]. Diffusion-action systems such as RDT further broaden the architecture families that may coexist in a deployment pool [Liu et al. 2024]. Composition methods such as MergeVLA combine compatible components inside a shared architecture [Fu et al. 2025]. RouterVLA instead keeps every expert frozen and architecture-agnostic. It asks what can be gained by coordinating the policies already available before training, merging, or distilling another one.

Problem Setup

We study *repeated-use commissioning*. A benchmark variant x denotes a fixed task-and-perturbation condition that receives a small probe budget before later scored executions. The setting therefore begins after the target condition is known but before the scored outcome is observed.

Experts and probe records. Let $\mathcal{E}$ be a frozen expert pool and $\mathcal{E}_x \subseteq \mathcal{E}$ the experts available for variant x. Each variant has recorded trials $\mathcal{T}_x$. For a scored trial $t \in \mathcal{T}_x$, expert e receives the probe set

$$P_{e,x}^{(t)} = \{r_{e,x,t'} : t' \in \mathcal{T}_x,\ t' \neq t\}, \tag{1}$$

where a record r contains success, rollout length, duration, and termination metadata. The outcome on trial t is excluded.

Commissioning profile. A profile map Φ converts the probe set and training-only expert metadata a_e into

$$\phi_e^{(t)}(x) = \Phi(P_{e,x}^{(t)}, a_e). \tag{2}$$

The metadata may include, for example, an expert success prior estimated from training suites, but never statistics from the held-out suite.

Selection and reward. A scorer assigns one value to each candidate,

$$s_{\theta,e}^{(t)}(x) = g_\theta\left(\phi_e^{(t)}(x)\right), \tag{3}$$

and selects

$$\hat{e}_\theta(x,t) = \arg\max_{e \in \mathcal{E}_x} s_{\theta,e}^{(t)}(x). \tag{4}$$

The notation includes deterministic rules by replacing g_θ with a fixed score such as empirical probe success. After selection, the recorded held-out reward is

$$R_\theta(x,t) = Y_{\hat{e}_\theta(x,t),x}^{(t)}, \qquad Y_{e,x}^{(t)} \in \{0,1\}. \tag{5}$$

For evaluation rows $\mathcal{I}$, the success rate is

$$\mathrm{SR}(\theta) = \frac{1}{|\mathcal{I}|} \sum_{(x,t)\in\mathcal{I}} R_\theta(x,t). \tag{6}$$

Realized upper reference. We report the hindsight success upper bound

$$U_x^{(t)} = \max_{e \in \mathcal{E}_x} Y_{e,x}^{(t)}. \tag{7}$$

This quantity asks whether any available expert succeeded on the recorded row after all outcomes are revealed. It is a realized Bernoulli upper reference, not an estimate of the best expert's true success probability, and it is not available to a deployed selector.

RouterVLA

RouterVLA is a commissioning-and-selection framework rather than a specialized neural architecture. Its common interface has two parts: a profile that records what is known about each candidate before the scored execution, and a selector that ranks the available profiles. This separation lets us measure the value of commissioning independently from the complexity of the decision rule.

Commissioning profiles

For each expert and variant we construct $\phi_e(x) \in \mathbb{R}^{14}$ from the probe set defined above; the trial superscript is omitted here for readability. We group the profile as

$$\phi_e = [S_e, R_e, P_e, M_e], \tag{8}$$

where S_e contains probe-success summaries, R_e contains rollout-trace summaries, P_e contains training-only priors, and M_e records probe count and missing statistics. Concretely, the profile includes empirical success, a Beta posterior mean and deviation, step-count and duration summaries, timeout and early-stop fractions, training-suite success and latency priors, probe count, and missing-statistic masks. The six trace features summarize rollout length, duration, timeout, and early termination. When a dispersion statistic cannot be estimated at the current budget, its numeric value is set to zero and the corresponding mask records that it is missing. The appendix lists all 14 features.

The full vector is a *commissioning profile*, not a behavior-only representation: explicit success evidence and training priors are separate from the rollout traces. This distinction matters because the experiments ask whether the traces add information after success is already known.

Transparent and learned selectors

Let c_e be the number of successful probes and B_e the number observed. The Empirical Probe Router ranks experts by

$$q_e^{\text{emp}} = c_e/B_e. \tag{9}$$

A uniform Beta$(1, 1)$ prior gives posterior mean

$$q_e^{\text{uni}} = \frac{1 + c_e}{2 + B_e}. \tag{10}$$

At equal $B_e = B$, this is a monotone transform of c_e/B and therefore induces the same ranking. The Hierarchical Beta-Binomial Router shrinks toward a training-suite prior μ_e,

$$q_e^{\text{hier}} = \frac{\tau\mu_e + c_e}{\tau + B_e}, \tag{11}$$

where the prior strength τ is tuned using training suites only. All transparent selectors break remaining ties with the training-suite prior and then a fixed expert-ID order. In the primary equal-budget audit, the three rules select the same expert on every evaluation row.

Learned selectors share a scalar function across experts,

$$s_{\theta,e}(x) = g_\theta(\phi_e(x)), \qquad \hat{e}_\theta(x) = \arg\max_{e \in \mathcal{E}_x} s_{\theta,e}(x). \tag{12}$$

We instantiate g_θ with logistic regression, gradient-boosted decision trees (GBDT), and a small MLP, $14 \to 64 \to 32 \to 1$. All three consume the same profiles and training examples. Their role is diagnostic as well as predictive: if richer trace summaries add useful information beyond success, a shared scorer should be able to preserve the success ranking while improving ambiguous cases.

Table 1: Evaluated LIBERO-Plus ledger and protocol.

Quantity	Value
Valid rollout records	34,752
Task-and-perturbation variants	398
Frozen expert IDs	28
Recorded trials per included pair	4
Variant–trial evaluation rows	1,592
Candidate count	mean 21.8; median 27
Candidate-count range	1–28
Rows with one candidate	0.8%
Primary split	3-to-1 trial-disjoint
Generalization split	leave-one-suite-out
Uncertainty	10,000 variant-cluster bootstraps

Training objective

Learned scorers train only on examples from the three non-held-out suites. For a training triple (x, t, e), the label is the disjoint recorded success $Y_{e,x}^{(t)}$. With

$$p_{\theta,e}^{(t)}(x) = \sigma\Big(g_\theta(\phi_e^{(t)}(x))\Big), \tag{13}$$

the MLP and logistic regression minimize binary cross entropy,

$$\mathcal{L}_{\text{BCE}}(\theta) = \frac{1}{|\mathcal{D}_{\text{train}}|} \sum_{(x,t,e)\in\mathcal{D}_{\text{train}}} \ell_{\text{BCE}}\Big(Y_{e,x}^{(t)}, p_{\theta,e}^{(t)}(x)\Big). \tag{14}$$

GBDT uses the same binary labels. The selector needs only the induced ranking, not calibrated probabilities. A loss ablation found no routing benefit from an additional listwise term, so all reported headline runs use the simpler BCE objective.

Experimental Protocol

The evaluation separates the evidence available at selection time from the outcome used to score that choice. All headline claims use trial-disjoint cross-fitting.

Ledger and candidate pool

The audited multi-platform ledger contains 34,960 rows. The quantitative study uses 34,752 valid rows from its LIBERO-Plus slice: 398 task-and-perturbation variants, four LIBERO suites, three perturbation axes, and 28 frozen expert IDs. Each included variant–expert pair has four recorded trial IDs, 0 through 3. The 200 non-LIBERO rows are excluded because they use a different expert pool. Table 1 summarizes the evaluated slice.

Candidate availability is part of the data rather than a post-hoc choice. The valid pool has mean size 21.8, median 27, and range 1–28; 0.8% of variants contain only one available expert. Every method ranks exactly the same valid set $\mathcal{E}_x$. At the default $B = 3$, exhaustive commissioning uses 65.5 probe executions on average for a target condition, with median 81 and range 3–84.

Trial-disjoint cross-fitting

For each variant x and scored trial $t \in \{0, 1, 2, 3\}$, profiles use the other three IDs, $\{0, 1, 2, 3\} \setminus \{t\}$. The selected expert is then scored on trial t. Rotating t yields

four folds per variant and 1,592 variant–trial evaluation rows. The rotation is symmetric: it uses every partition of three probe IDs and one scored ID. It guarantees outcome disjointness, but it is not a chronological deployment simulation because the trial IDs are ledger indices rather than physical timestamps.

Fold	Probe IDs	Scored ID
1	1,2,3	0
2	0,2,3	1
3	0,1,3	2
4	0,1,2	3

As a sensitivity check, we separately report the ID-ordered prefix row that uses IDs $\{0, 1, 2\}$ to score ID 3. It tests dependence on the symmetric rotation, not physical time ordering. A full diagram appears in Figure 2.

Generalization split and implementation

Learned scorers use leave-one-suite-out evaluation. For each held-out suite, the other three suites provide training examples; the MLP uses an internal 80/20 split by variant for early stopping. Scalers, expert priors, hierarchical shrinkage, and all hyperparameters are fit without held-out-suite information. The MLP result averages seeds 42, 123, 456, 789, and 1024. Logistic regression and GBDT use the same suite splits, profiles, and candidate masks. Implementation details are listed in Appendix Table 7.

Baselines, ties, and uncertainty

Global Best selects one expert using training-suite success and ignores target probes. The three commissioned success rules are defined above; after the final equivalence audit, they select the same expert on all 1,592 rows. The Hindsight bound sees all scored outcomes and is used only as a non-deployable upper reference.

Probe-success ties are resolved by training-suite prior and then a fixed expert-ID order. Learned score ties use the same final ID order. All choices are fixed before the scored outcome is read. Confidence intervals use 10,000 percentile bootstrap resamples clustered by variant ID, keeping all four folds, all methods, and all MLP seeds for a sampled variant together.

Same-trial evaluation appears only as an optimism diagnostic. It deliberately permits the scored trial to re-enter its own profile; those rows are never mixed with the main results or ablations.

Results

Unless stated otherwise, all results use the raw 14-dimensional profile and the 3-to-1 trial-disjoint protocol.

Commissioning turns a policy pool into a stronger system

Without target-specific evidence, Global Best succeeds on 0.4686 of scored executions. Three probes per available expert change that decision substantially: the transparent probe-success rule reaches 0.6149, a gain of 14.64 percentage points with 95% CI $[+11.37, +17.96]$. The realized Hindsight bound is 0.7393, confirming that the pool contains additional complementarity but also marking a non-deployable upper reference.

Table 2: Held-out success under trial-disjoint commissioning. Deltas and intervals are paired against Global Best.

Method	SR	Δ Global (pp)	95% CI
Global Best	0.4686	0.00	—
Probe-success rule	0.6149	+14.64	[+11.37,+17.96]
Logistic regression	0.6168	+14.82	[+11.49,+18.22]
GBDT	0.6187	+15.01	[+11.68,+18.40]
MLP	0.6144	+14.59	[+11.22,+18.02]
Hindsight upper bound	0.7393	+27.07	—

Notes. Empirical, Uniform-Beta, and tuned hierarchical success rules select the same expert on every primary evaluation row and are merged as the probe-success rule. GBDT differs from that rule by +0.38pp with paired 95% CI $[-0.88, +1.57]$.

Learned scorers recover the same level of performance. Logistic regression reaches 0.6168, GBDT 0.6187, and the MLP 0.6144. GBDT has the largest point estimate, but its paired difference from the transparent rule is only +0.38 points with 95% CI $[-0.88, +1.57]$. The main gain therefore comes from conditioning the choice on commissioning evidence, not from replacing a transparent decision with a more expressive scalar scorer. Table 2 reports the definitive values; Figure 3 visualizes the same comparison.

At three probes, success counts carry most of the scalar signal

Why does a count-based rule match learned models that also see timing, rollout length, termination, priors, and masks? At equal $B = 3$, the success count $c_e \in \{0, 1, 2, 3\}$ is already direct target-specific supervision. The uniform-Beta score is a monotone transformation of the same count, and the tuned hierarchical prior does not alter the final ranking. Under equal three-probe budgets with scalar-only profiles, binary probe success saturates the available routing signal. The learned models exploit correlations in the remaining features; these correlations improve aggregate success prediction but do not reliably change which expert is selected, because success counts already provide a strong ranking signal at $B = 3$.

The feature ablation makes this distinction precise. Inside the MLP, the full profile improves over Success+Prior by +1.07 points with 95% CI $[+0.10, +2.05]$. Behavior-only profiles also remain far above the permutation controls. Thus rollout traces contain predictive signal. Under this scalar-only information set, that signal overlaps substantially with the success evidence already present in the profile. Predicting success better in aggregate and choosing a better top-ranked expert

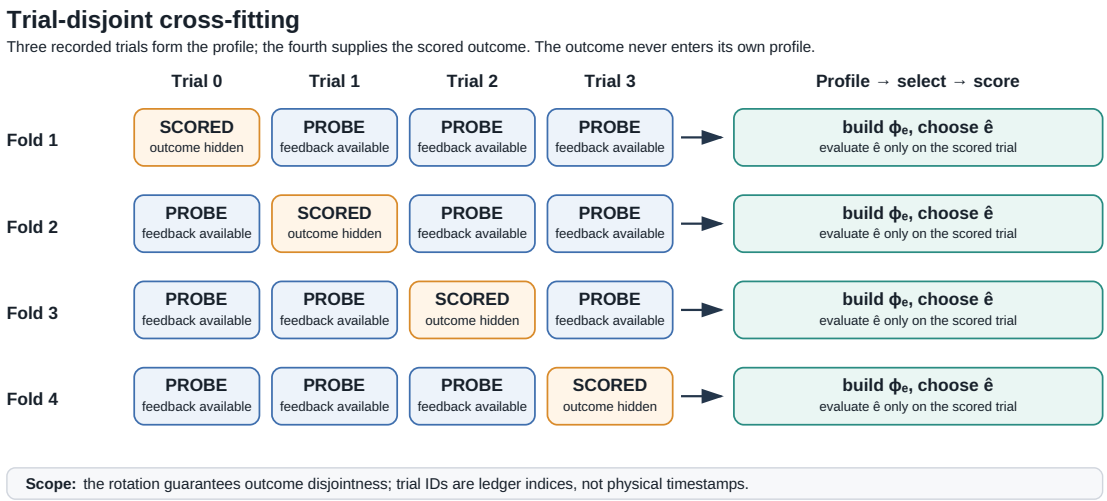

Figure 2: Four-fold trial-disjoint cross-fitting. Each row constructs profiles from three recorded trials and scores the selected expert on the fourth. The rotation guarantees outcome separation; trial IDs are ledger indices rather than physical timestamps.

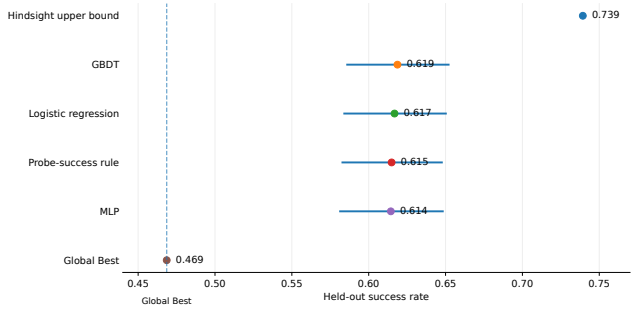

Figure 3: **Commissioning creates a large gain, while selector capacity changes little.** Points show held-out success. Horizontal intervals for commissioned and learned methods are paired 95% intervals against Global Best, shifted to the absolute success-rate axis. The Hindsight bound is a realized upper reference, not an available policy. Three-seed diagnostic values are reported separately in Table 3; this figure reports the primary main-result aggregates.

are not the same objective.

Outcome reuse can make routing look solved

The protocol changes the apparent answer. Within a dedicated matched protocol diagnostic, holding the profile builder, candidate mask, objective, seeds, and scorer fixed across the compared splits, same-trial reuse raises the MLP from 0.6132 to 0.7393—exactly the realized Hindsight bound. Measured relative to Global Best, the gain grows from +14.46 to +27.07 points, an inflation factor of 1.87 with 95% CI $[1.63, 2.24]$. The selector appears perfect because its own scored success is partially encoded in the profile.

Table 3: Which profile information matters? Values are from a three-seed MLP diagnostic.

Input groups	Held-out SR	Δ vs S+P (pp)
Prior only	0.4686	-13.65
Success only	0.6018	-0.33
Rollout traces only	0.6116	+0.65
Success + prior	0.6051	0.00
Rollout traces + prior	0.6200	+1.49
Full profile	0.6158	+1.07
Permuted profile	0.1011	-50.40

For the paired comparison Full − (Success+Prior), $\Delta = +1.07$pp with 95% CI $[+0.10, +2.05]$. Table 2 reports the primary five-seed MLP result.

The ID-ordered prefix diagnostic gives 0.6133 and +14.47 points over Global Best, close to the symmetric cross-fit result. Because the IDs are not timestamps, this is only a split sensitivity check; the defensible conclusion is outcome disjointness, not chronological generalization. Table 4 reports both diagnostics; the authoritative primary MLP aggregate in Table 2 is 0.6144.

The remaining bottleneck is evidence acquisition

Exhaustively probing every available expert is expensive. At $B = 3$, the primary pool requires 65.5 probe executions on average for one commissioned condition. A training-prior shortlist recovers much of the same accuracy with fewer probes: at $M = 12, B = 3$, logistic regression reaches 0.6185 with 36 probes; at $M = 3, B = 1$, it reaches 0.5597 with only three. The

Table 4: Protocol sensitivity within a dedicated matched MLP diagnostic.

Protocol	Held-out SR	Δ Global (pp)
Same-trial reuse	0.7393	+27.07
3-to-1 trial-disjoint	0.6132	+14.46
ID-prefix $\{0,1,2\}\to 3$	0.6133	+14.47

The gain inflation ratio is 1.87 with 95% CI $[1.63, 2.24]$. The primary MLP aggregate in Table 2 is 0.6144; the ratio above is computed entirely within this matched diagnostic. Trial IDs are ledger indices, so the prefix row is a split diagnostic rather than a chronological deployment test.

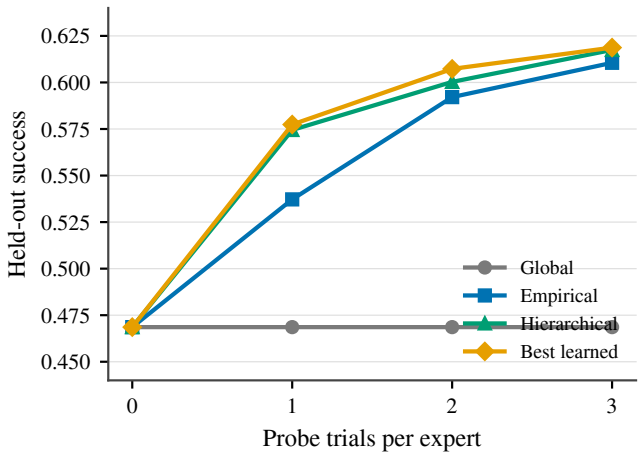

Figure 4: Probe-depth sensitivity under a common candidate pool. Additional probes improve every commissioned selector, while the no-probe Global Best baseline is flat; the curves converge by $B = 3$. The figure is a sensitivity diagnostic rather than a fresh-rollout learning curve.

probe-depth curve in Figure 4 shows the complementary effect of collecting more evidence per expert.

These results change the engineering question. If smoke tests are already required for qualification, the routing layer reuses a sunk cost. If probes are additional work, the useful design problem is not a larger scorer but a policy for choosing whom to test and when to stop. The full shortlist frontier and a cost accounting formula appear in the appendix.

Failure analysis: context and evidence

The two clearest failure modes call for different evidence. First, layout perturbations can change the visual arrangement without producing a distinctive scalar trace in only a few probes. The interpretation that missing visual context, rather than scorer capacity, explains the layout-axis gap is consistent with the data and motivates image-language routing experiments. Second, 59.2% of variant–trial rows contain a tie under probe success. Within the tied set, a learned behavior-based tie-break reaches 0.6083 versus 0.6072 for success plus prior, a difference of only 0.0011.

These patterns call for information rather than additional scorer capacity. Layout changes require observation context, while ties require more or better-allocated evidence. Table 5 summarizes the observed failure patterns and their interpretations. Both point beyond scalar scoring and toward the next decision problem: active commissioning.

Discussion

Routing as a second axis of scaling

The conventional scaling question is how to make one policy broader. RouterVLA asks a complementary systems question: how much capability can be extracted from a collection of policies before they are replaced by a better generalist? The answer in this ledger is substantial. Target-specific commissioning raises success by 14.64 points over one fixed expert even though the selector itself can be a count-based rule. The improvement comes from retaining conditional information that global model selection throws away.

This distinction matters for how the result should be read. The transparent rule is itself the core observation: when routine commissioning trials are preserved rather than collapsed into a global average, they reveal substantial conditional value. Under the trial-disjoint protocol, this value is measurable and large. Commissioning changes the information available to the routing decision, and that change accounts for most of the gain observed in this study.

Outcome separation as an evaluation principle

Complete ledgers are attractive because every counterfactual expert outcome is available for analysis. The same completeness makes it easy to build an impossible selector. Scored outcomes can leak through profile construction, normalization, candidate filtering, hyperparameter selection, or tie-breaking. Our same-trial diagnostic nearly doubles the measured gain and reaches the realized upper bound. A ledger-based routing study should therefore state the selector's information set before the scored execution and enforce that boundary mechanically. Outcome separation is part of the task, not an optional sensitivity check.

From model selection to a specialist lifecycle

Commissioning-aware routing suggests a persistent lifecycle rather than a one-time benchmark comparison:

$$\textsc{Onboard} \to \textsc{Commission} \to \textsc{Route} \to \textsc{Update} \to \textsc{Distill}.$$

The present experiments validate the Commission–Route link. The measured failure modes nevertheless make the next steps concrete. A useful system should shortlist experts, allocate probes where uncertainty remains, incorporate image-language context when traces

Table 5: Routing failure patterns and interpretations.

Regime	Observed pattern	Interpretation
Layout axis	No routing gain (MLP Δ negative on layout variants)	Layout changes call for image-language context beyond scalar behavior profiles
Low B	Lower success rate, more ties. $B = 1$ MLP SR ≈ 0.5837	More evidence or active probe allocation is the next decision problem
Equal B=3	Empirical/Hierarchical rules match learned scorers. 59.2% of rows are tied on probe success.	Under scalar-only profiles, binary success already carries most routing signal
Same-trial reuse	Matched MLP SR inflates from 0.6132 to 0.7393 (the realized Hindsight bound)	Outcome separation must exclude the scored trial from its own profile
Ties (59.2% of rows)	Learned tie-break SR is 0.6083 vs 0.6072 for success+prior	Behavioral traces add a small tie-breaking increment beyond success+prior

are ambiguous, and update profiles from subsequent routed executions. New experts could enter through the same black-box interface without exposing weights or sharing an architecture.

The longer-term opportunity is to treat a policy pool as a learning system rather than a temporary pile of checkpoints. Routed executions record where each expert earns trust and where the pool still fails. Those conditional trajectories may later help curate multi-teacher data for distillation into a generalist [Hinton et al. 2015], while selection quality and student quality remain distinct measurements. The present contribution supplies that first link: routine commissioning contains enough signal for the lifecycle to begin.

Limitations

The study uses a fixed LIBERO-Plus ledger with trial-disjoint cross-fitting, which establishes the Commission–Route link under a fully auditable information boundary. Natural next steps include fresh prequential rollouts that preserve physical time order and test the same routing decision under fatigue, drift, and environmental variation. Routing under layout changes calls for image-language context because scalar traces leave visual rearrangements ambiguous. Candidate availability is uneven; this motivates active probe allocation that decides which experts deserve another trial before the routed execution. When probes are extra work rather than sunk qualification cost, the shortlist frontier turns routing into a cost-sensitive design problem. These extensions follow directly from the measured failure modes and move the commissioning signal toward live deployment.

Conclusion

Robot learning usually treats smoke tests as a cost incurred before choosing a single global policy. Router-VLA shows that the same trials can support conditional expert selection when the scored outcome is kept outside the profile. Across 398 LIBERO-Plus variants, three probes per expert raise held-out success from 0.4686 to 0.6149. The strongest lesson is scoped: under equal three-probe budgets with scalar-only profiles, binary probe success saturates the available routing signal. Commissioning carries the value; extra scalar scorer capacity does not create it.

The second lesson is methodological. Reusing the scored trial inflates the measured gain by 1.87× and reaches the realized hindsight bound, so outcome separation must define any credible ledger-based routing task. Together, these findings change the next question from *how should we score a complete profile?* to *which evidence should we acquire, and when is it enough?*

Model scaling will continue to improve individual VLAs. Commissioning-aware routing offers a complementary way to improve the system assembled from them: test deliberately, preserve conditional evidence, and let deployment teach the selector where each expert earns trust. The experts will keep getting better; the system built from them should get better, too.

Acknowledgments. This work benefited from Agon [Sun et al. 2026a], an autonomous research system built on Prompt Economy [Sun et al. 2026b].

References

Johan Bjorck, Fernando Castañeda, Nikita Cherniadev, Xingye Da, Runyu Ding, Linxi Fan, et al. GR00T N1: An open foundation model for generalist humanoid robots, 2025. URL https://arxiv.org/abs/2503.14734.

Kevin Black, Noah Brown, Danny Driess, Adnan Esmail, Michael Robert Equi, Chelsea Finn, Niccolo Fusai, Lachy Groom, Karol Hausman, Brian Ichter, Szymon Jakubczak, Tim Jones, Liyiming Ke, Sergey Levine, Adrian Li-Bell, Mohith Mothukuri, Suraj Nair, Karl Pertsch, Lucy Xiaoyang Shi, Laura Smith, James Tanner, Quan Vuong, Anna Walling, Haohuan Wang, and Ury Zhilinsky. π_0: A vision-language-action flow model for general robot control. In *Proceedings of Robotics: Science and Systems*, 2025. doi: 10.15607/RSS.2025.XXI.010. URL https://arxiv.org/abs/2410.24164.

Anthony Brohan, Noah Brown, Justice Carbajal, Yev-

gen Chebotar, Xi Chen, Krzysztof Choromanski, Tianli Ding, Danny Driess, Avinava Dubey, Chelsea Finn, Pete Florence, Chuyuan Fu, Montse Gonzalez Arenas, Keerthana Gopalakrishnan, Kehang Han, Karol Hausman, Alexander Herzog, Jasmine Hsu, Brian Ichter, Alex Irpan, Nikhil Joshi, Ryan Julian, Dmitry Kalashnikov, Yuheng Kuang, Isabel Leal, Lisa Lee, Tsang-Wei Edward Lee, Sergey Levine, Yao Lu, Henryk Michalewski, Igor Mordatch, Karl Pertsch, Kanishka Rao, Krista Reymann, Michael Ryoo, Grecia Salazar, Pannag Sanketi, Pierre Sermanet, Jaspiar Singh, Anikait Singh, Radu Soricut, Huong Tran, Vincent Vanhoucke, Quan Vuong, Ayzaan Wahid, Stefan Welker, Paul Wohlhart, Jialin Wu, Fei Xia, Ted Xiao, Peng Xu, Sichun Xu, Tianhe Yu, and Brianna Zitkovich. RT-2: Vision-language-action models transfer web knowledge to robotic control, 2023a. URL https://arxiv.org/abs/2307.15818.

Anthony Brohan, Noah Brown, Justice Carbajal, Yevgen Chebotar, Joseph Dabis, Chelsea Finn, Keerthana Gopalakrishnan, Karol Hausman, Alex Herzog, Jasmine Hsu, Julian Ibarz, Brian Ichter, Alex Irpan, Tomas Jackson, Sally Jesmonth, Nikhil J. Joshi, Ryan Julian, Dmitry Kalashnikov, Yuheng Kuang, Isabel Leal, Kuang-Huei Lee, Sergey Levine, Yao Lu, Utsav Malla, Deeksha Manjunath, Igor Mordatch, Ofir Nachum, Carolina Parada, Jodilyn Peralta, Emily Perez, Karl Pertsch, Jornell Quiambao, Kanishka Rao, Michael Ryoo, Grecia Salazar, Pannag Sanketi, Kevin Sayed, Jaspiar Singh, Sumedh Sontakke, Austin Stone, Clayton Tan, Huong Tran, Vincent Vanhoucke, Steve Vega, Quan Vuong, Fei Xia, Ted Xiao, Peng Xu, Sichun Xu, Tianhe Yu, and Brianna Zitkovich. RT-1: Robotics transformer for real-world control at scale. In *Proceedings of Robotics: Science and Systems*, 2023b. doi: 10.15607/RSS.2023.XIX.025. URL https://doi.org/10.15607/RSS.2023.XIX.025.

Rui Cai et al. Xiaomi-Robotics-0: An open-sourced vision-language-action model with real-time execution, 2026. URL https://arxiv.org/abs/2602.12684.

Hao Chen et al. LaST-R1: Reinforcing robotic manipulation via adaptive physical latent reasoning, 2026a. URL https://arxiv.org/abs/2604.28192.

Yiteng Chen, Zhe Cao, Hongjia Ren, Chenjie Yang, Wenbo Li, Shiyi Wang, Yemin Wang, Li Zhang, Yanming Shao, Zhenjun Zhao, Huiping Zhuang, and Qingyao Wu. RoboRouter: Training-free policy routing for robotic manipulation, 2026b. URL https://arxiv.org/abs/2603.07892.

Senyu Fei, Siyin Wang, Junhao Shi, Zihao Dai, Jikun Cai, Pengfang Qian, Li Ji, Xinzhe He, Shiduo Zhang, Zhaoye Fei, Jinlan Fu, Jingjing Gong, and Xipeng Qiu. LIBERO-Plus: In-depth robustness analysis of vision-language-action models, 2025. URL https://arxiv.org/abs/2510.13626.

Matthias Feurer, Aaron Klein, Katharina Eggensperger, Jost Tobias Springenberg, Manuel Blum, and Frank Hutter. Efficient and robust automated machine learning. In *Advances in Neural Information Processing Systems*, volume 28, 2015. URL https://proceedings.neurips.cc/paper/2015/hash/11d0e6287202fced83f79975ec59a3a6-Abstract.html.

Yuxia Fu, Zhizhen Zhang, Yuqi Zhang, Zijian Wang, Zi Huang, and Yadan Luo. MergeVLA: Cross-skill model merging toward a generalist vision-language-action agent, 2025. URL https://arxiv.org/abs/2511.18810.

Geoffrey Hinton, Oriol Vinyals, and Jeff Dean. Distilling the knowledge in a neural network, 2015. URL https://arxiv.org/abs/1503.02531.

Nan Jiang and Lihong Li. Doubly robust off-policy value evaluation for reinforcement learning. In *Proceedings of the 33rd International Conference on Machine Learning*, pages 652–661, 2016. URL https://proceedings.mlr.press/v48/jiang16.html.

Jared Kaplan, Sam McCandlish, Tom Henighan, Tom B. Brown, Benjamin Chess, Rewon Child, Scott Gray, Alec Radford, Jeffrey Wu, and Dario Amodei. Scaling laws for neural language models, 2020. URL https://arxiv.org/abs/2001.08361.

Moo Jin Kim, Karl Pertsch, Siddharth Karamcheti, et al. OpenVLA: An open-source vision-language-action model, 2024. URL https://arxiv.org/abs/2406.09246.

Moo Jin Kim, Chelsea Finn, and Percy Liang. Fine-tuning vision-language-action models: Optimizing speed and success, 2025. URL https://arxiv.org/abs/2502.19645.

Dmytro Kuzmenko and Nadiya Shvai. MoIRA: Modular instruction routing architecture for multi-task robotics, 2025. URL https://arxiv.org/abs/2507.01843.

Lisha Li, Kevin Jamieson, Giulia DeSalvo, Afshin Rostamizadeh, and Ameet Talwalkar. Hyperband: A novel bandit-based approach to hyperparameter optimization. *Journal of Machine Learning Research*, 18(185):1–52, 2018. URL https://jmlr.org/papers/v18/16-558.html.

Qixiu Li, Yaobo Liang, Zeyu Wang, et al. CogACT: A foundational vision-language-action model for synergizing cognition and action in robotic manipulation, 2024. URL https://arxiv.org/abs/2411.19650.

Bo Liu, Yifeng Zhu, Chongkai Gao, Yihao Feng, Qiang Liu, Yuke Zhu, and Peter Stone. Libero: Benchmarking knowledge transfer for lifelong robot learning. In *Advances in Neural Information Processing Systems*, volume 36, pages 44776–44791, 2023. URL https://proceedings.neurips.cc/paper_files/paper/2023/hash/8c3c666820ea055a77726d66fc7d447f-Abstract-Datasets_and_Benchmarks.html.

Songming Liu, Lingxuan Wu, Bangguo Li, Hengkai Tan, Huayu Chen, Zhengyi Wang, Ke Xu, Hang Su, and Jun Zhu. RDT-1B: a diffusion foundation model for bimanual manipulation, 2024. URL https://arxiv.org/abs/2410.07864.

Octo Model Team, Dibya Ghosh, Homer Walke, Karl Pertsch, Kevin Black, Oier Mees, Sudeep Dasari, Joey Hejna, Tobias Kreiman, Charles Xu, Jianlan Luo, You Liang Tan, Lawrence Yunliang Chen, Pannag Sanketi, Quan Vuong, Ted Xiao, Dorsa Sadigh, Chelsea Finn, and Sergey Levine. Octo: An open-source generalist robot policy. In *Proceedings of Robotics: Science and Systems*, 2024. doi: 10.15607/RSS.2024.XX.090. URL https://doi.org/10.15607/RSS.2024.XX.090.

Isaac Ong, Amjad Almahairi, Vincent Wu, Wei-Lin Chiang, Tianhao Wu, Joseph E. Gonzalez, M. Waleed Kadous, and Ion Stoica. RouteLLM: Learning to route llms with preference data, 2024. URL https://arxiv.org/abs/2406.18665.

Open X-Embodiment Collaboration et al. Open X-Embodiment: Robotic learning datasets and RT-X models. In *2024 IEEE International Conference on Robotics and Automation (ICRA)*, pages 6892–6903, 2024. doi: 10.1109/ICRA57147.2024.10611477. URL https://arxiv.org/abs/2310.08864.

Adam Paszke, Sam Gross, Francisco Massa, Adam Lerer, James Bradbury, Gregory Chanan, Trevor Killeen, Zeming Lin, Natalia Gimelshein, Luca Antiga, Alban Desmaison, Andreas Köpf, Edward Yang, Zachary DeVito, Martin Raison, Alykhan Tejani, Sasank Chilamkurthy, Benoit Steiner, Lu Fang, Junjie Bai, and Soumith Chintala. PyTorch: An imperative style, high-performance deep learning library. In *Advances in Neural Information Processing Systems*, volume 32, 2019. URL https://proceedings.neurips.cc/paper/2019/hash/bdbca288fee7f92f2bfa9f7012727740-Abstract.html.

Fabian Pedregosa, Gaël Varoquaux, Alexandre Gramfort, Vincent Michel, Bertrand Thirion, Olivier Grisel, Mathieu Blondel, Peter Prettenhofer, Ron Weiss, Vincent Dubourg, Jake Vanderplas, Alexandre Passos, David Cournapeau, Matthieu Brucher, Matthieu Perrot, and Édouard Duchesnay. Scikit-learn: Machine learning in python. *Journal of Machine Learning Research*, 12:2825–2830, 2011. URL https://jmlr.org/papers/v12/pedregosa11a.html.

Physical Intelligence, Kevin Black, Noah Brown, James Darpinian, Karan Dhabalia, Danny Driess, Adnan Esmail, Michael Equi, Chelsea Finn, Niccolo Fusai, Manuel Y. Galliker, Dibya Ghosh, Lachy Groom, Karol Hausman, Brian Ichter, Szymon Jakubczak, Tim Jones, Liyiming Ke, Devin LeBlanc, Sergey Levine, Adrian Li-Bell, Mohith Mothukuri, Suraj Nair, Karl Pertsch, Allen Z. Ren, Lucy Xiaoyang Shi, Laura Smith, Jost Tobias Springenberg, Kyle Stachowicz, James Tanner, Quan Vuong, Homer Walke, Anna Walling, Haohuan Wang, Lili Yu, and Ury Zhilinsky. $\pi_{0.5}$: a vision-language-action model with open-world generalization, 2025. URL https://arxiv.org/abs/2504.16054.

John R. Rice. The algorithm selection problem. *Advances in Computers*, 15:65–118, 1976. doi: 10.1016/S0065-2458(08)60520-3. URL https://doi.org/10.1016/S0065-2458(08)60520-3.

StarVLA Community. StarVLA: A lego-like codebase for vision-language-action model developing, 2026. URL https://arxiv.org/abs/2604.05014.

Youran Sun, Xingyu Ren, Chugang Yi, Jiaxuan Guo, Kejia Zhang, Jianda Du, and Haizhao Yang. Agon: An autonomous large-scale omnidisciplinary research system built on prompt economy, 2026a. URL https://arxiv.org/abs/2606.24177.

Youran Sun, Xingyu Ren, Kejia Zhang, Xinpeng Liu, and Jiaxuan Guo. Perspectivegap: A benchmark for multi-agent orchestration prompting, 2026b. URL https://arxiv.org/abs/2606.08878.

Philip S. Thomas and Emma Brunskill. Data-efficient off-policy policy evaluation for reinforcement learning. In *Proceedings of the 33rd International Conference on Machine Learning*, pages 2139–2148, 2016. URL https://proceedings.mlr.press/v48/thomasa16.html.

Chris Thornton, Frank Hutter, Holger H. Hoos, and Kevin Leyton-Brown. Auto-WEKA: Combined selection and hyperparameter optimization of classification algorithms. In *Proceedings of the ACM SIGKDD International Conference on Knowledge Discovery and Data Mining*, pages 847–855, 2013. doi: 10.1145/2487575.2487629. URL https://doi.org/10.1145/2487575.2487629.

Yihao Wang, Pengxiang Ding, Lingxiao Li, Can Cui, Zirui Ge, Xinyang Tong, Wenxuan Song, Han Zhao, Wei Zhao, Pengxu Hou, Siteng Huang, Yifan Tang, Wenhui Wang, Ru Zhang, Jianyi Liu, and Donglin Wang. VLA-Adapter: An effective paradigm for tiny-scale vision-language-action model, 2025. URL https://arxiv.org/abs/2509.09372.

Ronald J. Williams. Simple statistical gradient-following algorithms for connectionist reinforcement learning. *Machine Learning*, 8:229–256, 1992. doi: 10.1007/BF00992696. URL https://doi.org/10.1007/BF00992696.

Xiao-Ming Wu, Bin Fan, Kang Liao, Jian-Jian Jiang, Runze Yang, Yihang Luo, Zhonghua Wu, Wei-Shi Zheng, and Chen Change Loy. VLANeXt: Recipes for building strong vla models, 2026. URL https://arxiv.org/abs/2602.18532.

Jinliang Zheng, Jianxiong Li, Zhihao Wang, Dongxiu Liu, Xirui Kang, et al. X-VLA: Soft-prompted transformer as scalable cross-embodiment vision-language-action model, 2025. URL https://arxiv.org/abs/2510.10274.

Table 6: The 14 raw commissioning-profile features used by learned scorers.

Group	Features
S: success	empirical success mean; uniform-Beta posterior mean; posterior standard deviation
R: rollout traces	step mean; step standard deviation; duration mean; duration standard deviation; timeout fraction; early-stop fraction
P: prior	training-suite expert success prior; training-suite latency prior
M: availability	probe count; missing-mean mask; missing-standard-deviation mask

Table 7: Fixed settings for the primary learned-scorer comparison.

Setting	Value
MLP	$14 \to 64 \to 32 \to 1$
Optimizer	Adam
Learning rate	10^{-3}
Weight decay	10^{-4}
Batch size	256
Objective	binary cross entropy
Epoch cap	500
Early stopping patience	50
MLP seeds	42, 123, 456, 789, 1024
Bootstrap	10,000, clustered by variant

Appendix: Supplementary Details

A. Ledger filtering and units

The audited ledger contains 34,960 rows across all recorded platforms. The main evaluation retains 34,752 valid rows from the LIBERO-Plus slice after platform filtering, validity checks, and removal of incomplete variant–expert records. Those rows cover 398 variants, four suites, three perturbation axes, 28 expert IDs, and four recorded trials per included variant–expert pair. The four-way trial rotation produces 1,592 variant–trial evaluation rows. The 200 non-LIBERO rows are excluded from quantitative claims because their expert pool is not comparable.

A row with $K = 1$ contributes to the aggregate success rate but contains no routing choice; such variants account for 0.8% of the evaluated set. All methods use the same candidate mask on every variant–trial row.

B. Profile features

C. Learned-scorer settings

Logistic regression uses standardized profiles with $C = 1.0$. GBDT uses 20 boosting iterations, maximum depth 5, 32 bins, and early stopping. The implementations use PyTorch [Paszke et al. 2019] and scikit-learn [Pedregosa et al. 2011].

D. Expert pool

Table 8 lists every expert that appears in the evaluated LIBERO-Plus ledger, together with its architecture family, approximate parameter scale when recorded, and the trials available for commissioning.

The pool spans flow-matching ($\pi_{0.5}$), diffusion (RDT-1B), autoregressive (OpenVLA, VLANeXt, StarVLA), and modular (CogACT, MergeVLA, VLA-Adapter, LaST-R1) architectures. Suite-specific rows are experts fine-tuned for a single LIBERO suite; their near-zero cross-suite rates confirm specialization. The complementarity is structural: the top overall expert ($\pi_{0.5}$, 0.507) is not the top expert on Object or Spatial, and the suite specialists achieve their best numbers precisely where generalists are weakest. — means the suite was not evaluated for that expert (0 rows). 0.000 means the expert was tested (1,280 rows) but recorded zero successes. VLA-Adapter (object) has 960 rows because its Long-suite deployment did not complete; the other three VLA-Adapter variants have complete four-suite coverage. Suite-specific checkpoints were primarily deployed on their target suite, with cross-suite rows reflecting off-target evaluation.

E. Shortlist frontier

The shortlist is selected from training-suite priors before target probes are observed. Mean probe count is therefore $M \times B$.

F. Probe-cost accounting

When probe executions are additional work rather than part of normal model qualification, their cost must be amortized over repeated use. For a selector π, deployment horizon H, and probe-to-scored-execution cost ratio ρ, we report the diagnostic

$$J(\pi; H, \rho) = H \cdot \mathrm{SR}(\pi) - \rho C_{\mathrm{probe}}. \tag{15}$$

For a commissioned condition x,

$$C_{\mathrm{probe}}(x) = B\,|\mathcal{E}_x^{\mathrm{probe}}|, \tag{16}$$

and the reported cost is averaged over variants. The full-pool $B = 3$ setting uses 65.5 probes on average because candidate availability varies. If the smoke tests would be run regardless of routing, the incremental probe cost is instead approximately zero; these are distinct deployment scenarios.

G. Visual context

Table 8: Expert pool evaluated in the LIBERO-Plus trial-disjoint experiments. — marks unevaluated suites (no data); 0.000 means tested but zero successes. The complementarity pattern—no single expert dominates all suites—creates the headroom that commissioning-aware routing exploits.

Model	HuggingFace / Source	Object	Spatial	Long	Goal	Overall
$\pi_{0.5}$ (excluded from routing pool)	`physical-intelligence/pi0.5` [Physical Intelligence et al. 2025]	**0.644**	**0.759**	**0.384**	**0.241**	**0.507**
X-VLA	`2toINF/X-VLA-Libero` [Zheng et al. 2025]	0.397	0.688	0.359	0.206	0.413
OpenVLA-OFT	`Sylvest/openvla-7b-oft-finetuned-libero-plus-mixdata` [Kim et al. 2025]	0.422	0.444	0.188	0.238	0.323
DB-CogACT	`CogACT/CogACT-Base` [Li et al. 2024]	0.431	0.497	0.197	0.116	0.310
Xiaomi Robotics-0	`Xiaomi-robotics-0` [Cai et al. 2026]	0.331	0.469	0.156	0.066	0.256
MergeVLA-LoRA (object)	`FYX026/MergeVLA-LIBERO` [Fu et al. 2025]	0.613	0.000	0.000	0.000	0.153
StarVLA	`StarVLA/Qwen3-VL-OFT-...` [StarVLA Community 2026]	0.122	0.384	0.022	0.047	0.144
MergeVLA-LoRA (spatial)	`FYX026/MergeVLA-LIBERO` [Fu et al. 2025]	0.000	0.569	0.000	0.000	0.142
GR00T N1	`nvidia/gr00t-n1` [Bjorck et al. 2025]	0.256	0.228	0.009	0.069	0.141
VLA-Adapter (spatial)	`VLA-Adapter/LIBERO-Spatial-Pro` [Wang et al. 2025]	0.000	0.559	0.000	0.000	0.140
VLANeXt	`DravenALG/VLANeXt` [Wu et al. 2026]	0.031	0.206	0.066	0.113	0.104
OpenVLA-LoRA	`openvla/openvla-7b` + LoRA [Kim et al. 2024]	0.100	0.194	0.003	0.007	0.078
OpenVLA	`openvla/openvla-7b` [Kim et al. 2024]	0.050	0.184	0.013	0.003	0.063
VLA-Adapter (object)	`VLA-Adapter/LIBERO-Object-Pro` [Wang et al. 2025]	0.184	0.000	—	0.000	0.062
LaST-R1 (object)	`chenhao01/LaST-R1` [Chen et al. 2026a]	0.188	0.000	0.000	0.000	0.047
MergeVLA-LoRA (long)	`FYX026/MergeVLA-LIBERO` [Fu et al. 2025]	0.000	0.000	0.156	0.000	0.039
MergeVLA-LoRA (goal)	`FYX026/MergeVLA-LIBERO` [Fu et al. 2025]	0.000	0.000	0.000	0.141	0.035
LaST-R1 (long)	`chenhao01/LaST-R1` [Chen et al. 2026a]	0.000	0.009	0.078	0.003	0.023
VLA-Adapter (goal)	`VLA-Adapter/LIBERO-Goal-Pro` [Wang et al. 2025]	0.000	0.000	0.000	0.075	0.019
VLA-Adapter (long)	`VLA-Adapter/LIBERO-Long-Pro` [Wang et al. 2025]	0.000	0.000	0.041	0.000	0.010
LaST-R1 (goal)	`chenhao01/LaST-R1` [Chen et al. 2026a]	0.000	0.000	0.000	0.034	0.009

Table 9: Frozen top-M shortlist frontier. Values are held-out success rates under trial-disjoint evaluation.

M	B	Probes	Global Best	Uniform-Beta	Hierarchical	Logistic
3	1	3	0.4686	0.5265	0.5553	0.5597
3	2	6	0.4686	0.5735	0.5775	0.5796
3	3	9	0.4686	0.5879	0.5961	0.5959
5	1	5	0.4686	0.5174	0.5635	0.5679
5	2	10	0.4686	0.5759	0.5884	0.5906
5	3	15	0.4686	0.5942	0.6062	0.6072
8	1	8	0.4686	0.5373	0.5712	0.5752
8	2	16	0.4686	0.5947	0.5960	0.5980
8	3	24	0.4686	0.6080	0.6112	0.6118
12	1	12	0.4686	0.5372	0.5745	0.5774
12	2	24	0.4686	0.5921	0.6003	0.6025
12	3	36	0.4686	0.6106	0.6175	0.6185

LIBERO suite overview

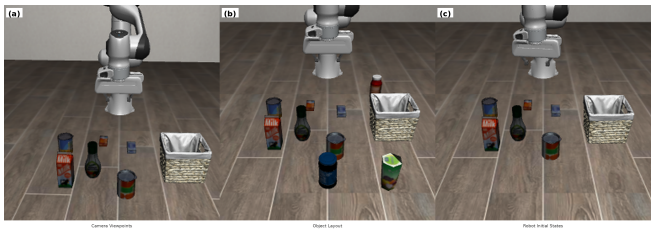

Perturbation axes

Figure 5: Visual context for the evaluated LIBERO-Plus ledger. These images illustrate suites and perturbations; they are not inputs to the current selectors and are not evidence for expert complementarity.